Experimental response of headed stud connections subjected to combined shear and bending actions

Otgonchimeg Davaadorj, Paolo M. Calvi, and John F. Stanton

- This paper presents the results of an experimental program investigating the effects of load eccentricity and stud distribution on headed stud connections subjected to combinations of shear and bending actions.
- The program included five test specimens that were representative of precast concrete beam-to-column joints.

PCI Journal (ISSN 0887-9672) V. 65, No. 5, September–October 2020.
PCI Journal is published bimonthly by the Precast/Prestressed Concrete Institute, 8770 W. Bryn Mawr Ave., Suite 1150, Chicago, IL 60631.

Embedded steel plates anchored by welded studs are commonly used in precast concrete construction to support welded field plates that connect members. The research reported here addresses the capacity of groups of embedded studs subjected to loading in flexure and shear.

Headed stud connections have received considerable research attention over the past 60 years.[1–7] These research programs produced a significant amount of data and led to the development of behavioral models that have been implemented in code recommendations for resistance to shear loading. For instance, the work of Ollgaard et al.[5] forms the basis for the American Institute of Steel Construction (AISC) design equations.[8]

The great majority of the research on welded studs has focused on composite beam behavior and used push-off specimens consisting of a wide flange beam section placed between two concrete slabs (**Fig. 1**). Headed studs were welded to both flanges and embedded in the surrounding concrete slab elements. Axial forces applied to the beam cross section caused pure shear in the welded studs. Parameters investigated in these studies included the h_s/d_s ratio (that is, the ratio between the stud length and its diameter), the number and distribution of studs, the concrete strength and density, and the slab thickness.

Only a relatively small number of studies have been conducted on connections representative of precast concrete applications. Furthermore, most of the steel beam push-

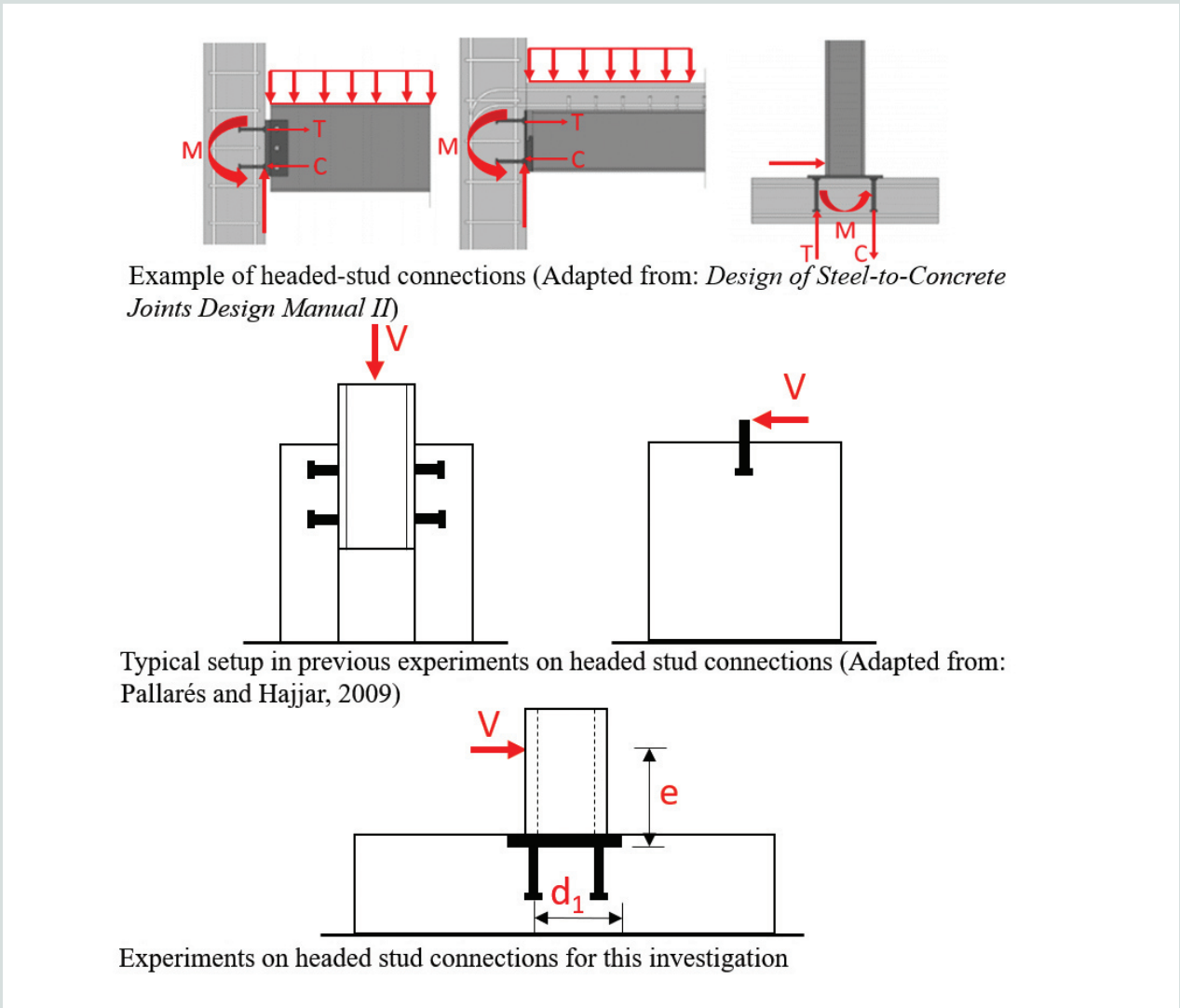

Figure 1. Headed stud connections. Note: C = compression force; d_1 = distance of studs in row 1 from embed plate edge; e = load eccentricity; M = moment; T = tensile force; V = shear force.

off tests have characteristics that limit their applicability to typical precast concrete connections. For example, few of them included studs placed close enough to a free edge that concrete edge breakout was possible.

In response to this, PCI launched a comprehensive research study involving an extensive experimental program, aimed at expanding the database of headed stud test results.[9] The variables considered in that experimental program included front-edge distance, corner conditions, side-edge distance, and rear-edge distance. In addition, some studies were conducted to evaluate the effects of combined tension and shear on a group of headed studs. The study provided invaluable experimental evidence and a better understanding of headed stud connections and also resulted in some modifications of the provisions given in the *PCI Design Handbook: Precast and Prestressed Concrete*.[10] Despite these advances, very few studies have addressed the influence of simultaneous shear and bending on connection behavior, even though it is considered an important parameter.[11]

Figure 1 provides some examples of common headed stud connections. As shown in the figure, the applied loads generate combinations of shear and bending that need to be effectively transferred across the plate-to-concrete interface to the adjacent structural element.

Although there is evidence suggesting that the transfer of shear forces across a steel-to-concrete plane crossed by headed studs occurs through a combination of friction and dowel action (and possibly cohesion), there is still no agreement about the way in which these resisting mechanisms share the applied loads. The range of different design approaches extant today (such as those of the American Association of State Highway and Transportation Officials [AASHTO], American Concrete Institute [ACI], PCI, and AISC) illustrates the

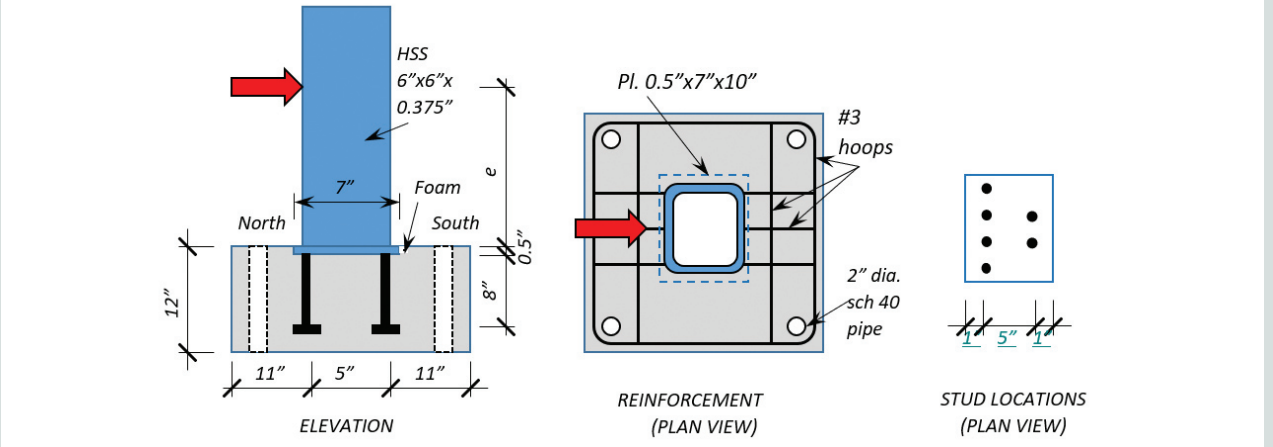

Figure 2. Test specimen details. Note: *e* = load eccentricity; HSS = hollow structural section. No. 3 = 10M; 1" = 1 in. = 25.4 mm.

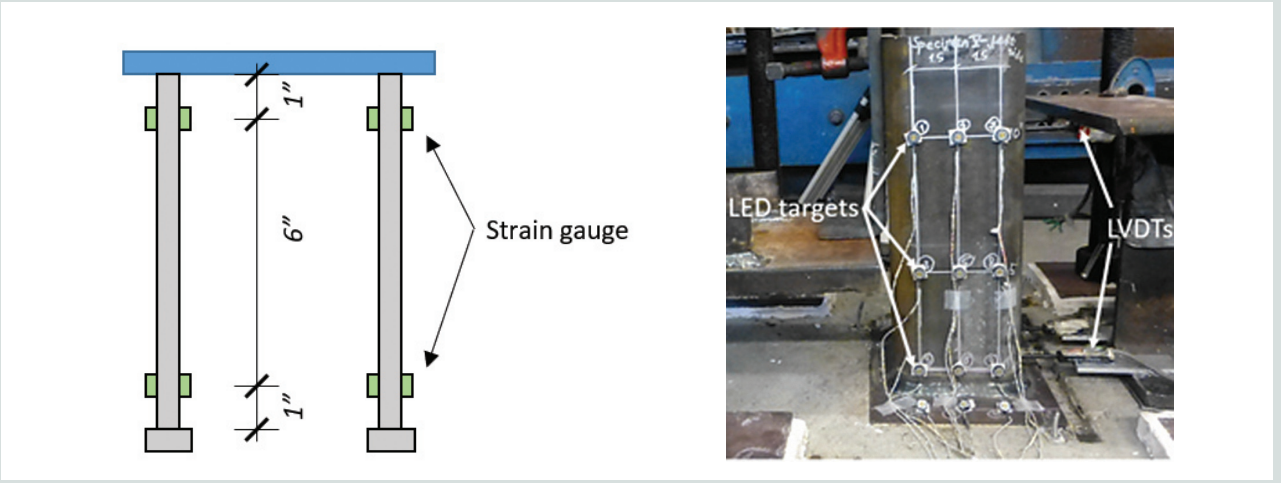

Figure 3. Test instrumentation. Note: LED = light-emitting diode; LVDT = linear variable displacement transducer. 1" = 1 in. = 25.4 mm.

point.[8,10,12,13] For instance, ACI 318-14 states that headed stud connections can either be designed using the shear friction provisions in chapter 22.9 or the anchoring-to-concrete provisions in chapter 17. When no studs are used and shear force is transferred by cohesion alone, such as for topping slabs on precast concrete members, the connection may be designed by the interface shear transfer provisions in chapter 16. The *PCI Design Handbook* contains recommendations very similar to those of chapter 17 of ACI 318-14.

According to the shear friction theory (ACI 318-14 chapter 22.9), the steel studs or bars crossing the shear plane resist only tension and the shear strength of the connection is attributed entirely to friction, made possible by the corresponding normal compression force. In contrast, the design approach reported in chapter 17 states that the studs act in shear alone and provide the entire shear strength of the connection, with no tension in the studs and no friction at the interface. These are two diametrically opposing views of the sources of the studs' shear resistance. Although in some instances those models produce similar results, they may also lead to very different outcomes, particularly when a moment acts in addition to a shear force. Consequently, there is a need to develop a satisfactory explanation of the local load-resisting mechanisms so that the loads can be distributed rationally between them for purposes of design.

The purpose of this study is to provide experimental evidence and some better insight into the response of headed stud connections subjected to monotonic combinations of shear and bending. To this end, a test program was planned and conducted in the Structural Research Laboratory at the University of Washington in Seattle. The experimental program involved a total of five specimens (Fig. 1), which are described in detail in later sections. The main variables considered were the mo-

ment-to-shear ratio and the stud distribution across the steel plate. All specimens were heavily instrumented, and strain, displacement, and force data were continuously recorded throughout each test.

Experimental program

In the experimental program, the test specimens were designed to ensure that premature failure did not occur outside the interface between the steel plate and the concrete, and to allow the shear and normal stresses across the interface to be accurately computed.

Figures 2 and **3** show details of the specimens and instrumentation. The concrete had f'_c compressive strength of approximately 7000 psi (48.3 MPa) on the day of testing.

Concrete breakout mechanisms were outside the scope of this work, so the properties of the studs were selected to prevent them. The literature shows that elements with slender studs ($h_s/d_s > 4.5$, for normalweight concrete) tend to experience stud failure.[14] The studs selected for the tests had $d_s = \frac{5}{8}$ in. (15.875 mm) and $h_s = 8$ in. (203.2 mm), giving $h_s/d_s = 12.8$. They were welded in accordance with the American Welding Society's AWS D1.1.[15] Three stud samples were tested in tension. **Figure 4** shows the resulting stress-strain curves. The three tests showed almost identical results, with ultimate tensile strength of stud anchors f_{uta} = 81 ksi (558.5 MPa).

To eliminate any bearing contribution of the concrete in the front of the plate, foam strips (11 in. [279.4 mm] wide) were attached to the south side of the embed plate, opposite the position of the actuator.

A 110 kip (489 kN) hydraulic actuator applied the load to the HSS loading post through a series of steel plates, which were used to achieve different load eccentricities.

All specimens were subjected to monotonically increasing horizontal loads to failure (the tests were stopped once the applied load started to drop after reaching peak load). Three different load eccentricities were considered throughout the experimental program, namely e = 1.5, 3, and 5.5 in. (38.1, 76.2, and 139.7 mm), measured from the bottom of the embed plate to the point of application of the horizontal load. These values were selected to give a relatively wide range of e/d_1 ratios (where d_1 is the distance between the first row, or north studs, and the south edge of the embed plate) while being representative of connections typical of precast concrete beam-to-column/wall joints, in which the load eccentricity is relatively small.

Table 1 gives a summary of the characteristics of the five experiments. The specimen names contain three identifiers:

- the number of studs in the first row n_1
- the number of studs in the second row n_2
- the ratio e/d_1

Thus specimen 4-0-0.92 indicates four studs in the first row (upstream or closest to the loading actuator), no studs in the second row, and $e/d_1 = 0.92$. The listed concrete strengths are the average of three 6 × 12 in. (152.4 × 304.8 mm) cylinders tested on the day of specimen loading, which was generally about 40 days after casting.

Figure 3 shows the instrumentation setup. All specimens were heavily instrumented. Strain gauges were attached to the shear studs at various locations to monitor flexural and axial strains and consequently calculate the stud forces. Light-emitting diode (LED) targets were attached to both the plate and the loading post and were tracked using a motion capture system to monitor plate displacements, rotations, and the like in three dimensions. Finally, two pairs of linear

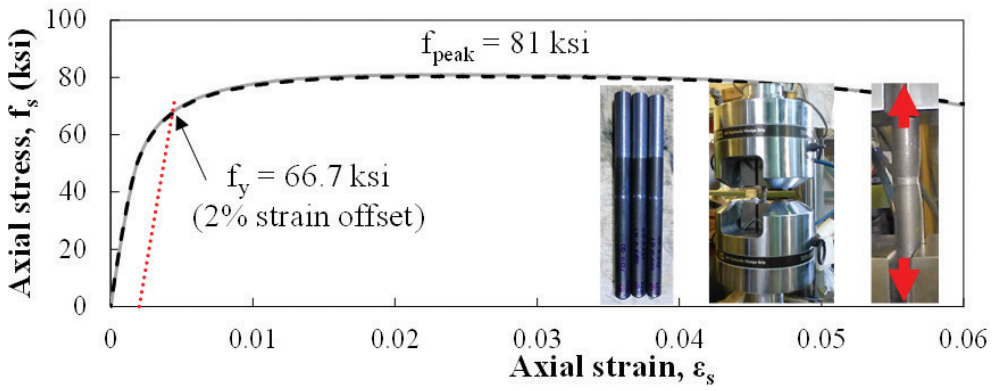

Figure 4. Stud steel stress-strain curve. Note: f_{peak} = peak tensile stress of studs obtained from tension test; f_y = stud yield stress obtained from tension test. 1 ksi = 6.895 MPa.

Table 1. Test characteristics

Specimen ID	f_c', psi	n_1	n_2	e, in.	d_1, in.	e/d_1
2-0-0.92	7589	2	0	5.5	6	0.92
4-0-0.92	7545	4	0	5.5	6	0.92
2-2-0.92	7627	2	2	5.5	6	0.92
2-2-0.25	7667	2	2	1.5	6	0.25
2-2-0.50	7749	2	2	3.0	6	0.50

Note: d_1 = distance of studs in row 1 from embed plate edge; e = load eccentricity; f_c' = concrete compressive strength; n_1 = numbers of studs in row 1; n_2 = number of studs in row 2. 1 in. = 25.4 mm; 1 psi = 6.895 kPa.

Table 2. Test results

Specimen ID	V_{test}, kip	Δ_{test}, in.	w_u, in.	α_u, rad
2-0-0.92	39.20	0.51	0.195	0.054
4-0-0.92	76.80	0.56	0.20	0.058
2-2-0.92	38.68	0.19	0.36	0.070
2-2-0.50	83.86	0.32	0.11	0.019
2-2-0.25	84.15	0.46	0.32	0.067

Note: V_{test} = total applied shear force applied in test; w_u = separation between steel plate and concrete at ultimate shear load; α_u = plate rotation at ultimate shear load; Δ_{test} = plate horizontal displacement at peak load. 1 in. = 25.4 mm; 1 kip = 4.448 kN.

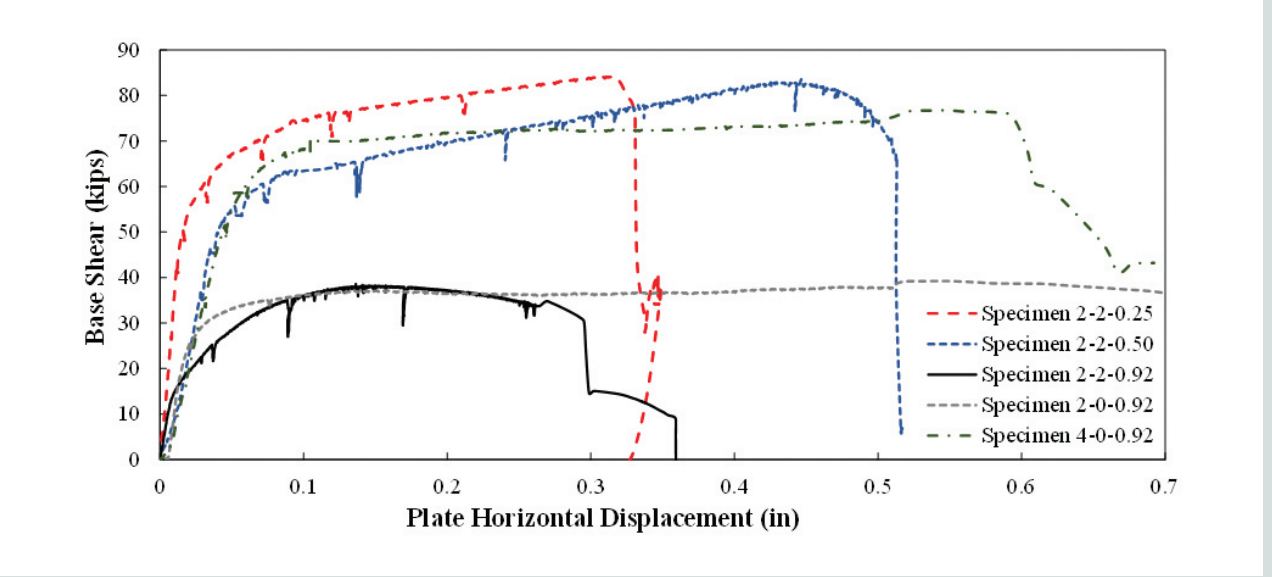

Figure 5. Interface shear versus plate displacement response of all specimens tested. Note: 1 in. = 25.4 mm; 1 kip = 4.448 kN.

variable displacement transformer displacement sensors were used to monitor the horizontal displacement of the top and bottom of the loading post.

Additional information (such as photographs and observable cracks) was documented throughout each test at selected load stages. The applied loads were monitored using a load cell. A pressure transducer mounted on the hydraulic line provided backup.

Experimental observations

The key experimental results are summarized in **Table 2**. **Figure 5** shows the load-displacement curves for all five specimens and illustrates the strength behavior. The displacement shown is that of the embed plate. **Figure 6** shows the rotation

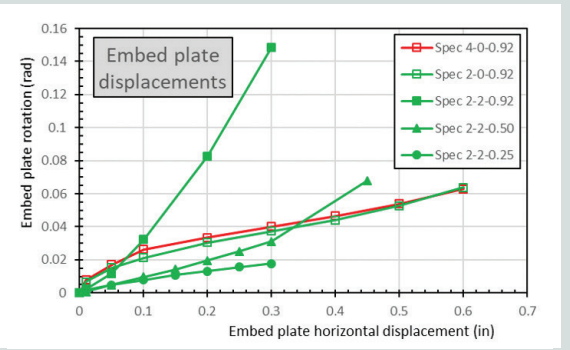

Figure 6. Embed plate slip displacement versus rotation. Note: 1 in. = 25.4 mm.

of the loading post as a function of the embed plate horizontal displacement and illustrates the kinematic behavior. As discussed more extensively in later sections, all specimens were selected to fall in a mixed response region, in which the embed plate experiences a combination of sliding and rotation. This scenario is commonly found in practice but leads to complex interface mechanics because the studs are subjected to a combination of shear and axial forces.

The fact that the studs were under a state of multiaxial stress was confirmed by the readings from the strain gauges attached to the studs, which indicated both axial and flexural/shear deformations, with relative magnitudes that varied among specimens. In those that predominantly experienced plate rotation, the strain gauges indicated that the studs were largely subjected to tension, with only minor bending deformations induced by applied shear. In contrast, in specimens that experienced significant horizontal slip, the gauge readings indicated more flexure relative to the amount of tension.

Effects of eccentricity

Figure 5 shows the load-displacement experimental response for three of the specimens tested, namely 2-2-0.25, 2-2-0.50, and 2-2-0.92. These three specimens were nominally identical, with two rows of two studs in each, and were subjected to monotonically increasing horizontal load with different eccentricities.

All three specimens experienced a stud failure with minor damage to the concrete block (minor cracking on the surface in the vicinity of the plate [**Fig. 7**]). In general, the embed plate slid and rotated as a rigid body with no observable bending deformation, as confirmed by the displacement profile obtained from the LED targets.

The effects of the load eccentricity on the response of the specimens were interpreted by comparing the curves shown in Fig. 6. First, Fig. 6 shows that larger load eccentricity leads to a larger ratio of rotation angle to slip distance at all loads. Although the kinematic behaviors of specimens 2-2-0.25 and 2-2-0.50 were quite similar, specimen 2-2-0.92 showed significantly more rotation. Figure 7 shows this finding, which is attributed to the larger eccentricity of the load.

Second, larger eccentricity leads to a lower failure load (Fig. 5). Specimens 2-2-0.25 and 2-2-0.50 failed at high loads, while 2-2-0.92, with its higher eccentricity, failed at a much lower load. In principle, this is to be expected because more of the connection's capacity must be devoted to resisting bending moment. However, as shown later, the strength of specimen 2-2-0.92 appears to be anomalously low. The fact that specimens 2-2-0.25 and 2-2-0.50 failed at similar loads, despite their different eccentricities (3 and 1.5 in. [76.2 and 38.1 mm], respectively) suggests that their eccentricities were low enough to have little influence on the failure load. The main differences lie in their ultimate displacements. (The measured elastic stiffness of specimen 2-2-0.25 was also higher, but this information is of questionable value because the elastic behavior depends on the details of contact between the studs and the concrete and those contact details are sensitive to matters such as the exact degree of consolidation of the concrete around the studs.)

Effects of stud distribution

Three of the tested specimens had different stud distributions. Specimens 2-0-0.92 and 4-0-0.92 had a single row of two- and four-headed studs, respectively, centered 1 in. (25.4 mm) from the north edge of the plate, hence on the tension side

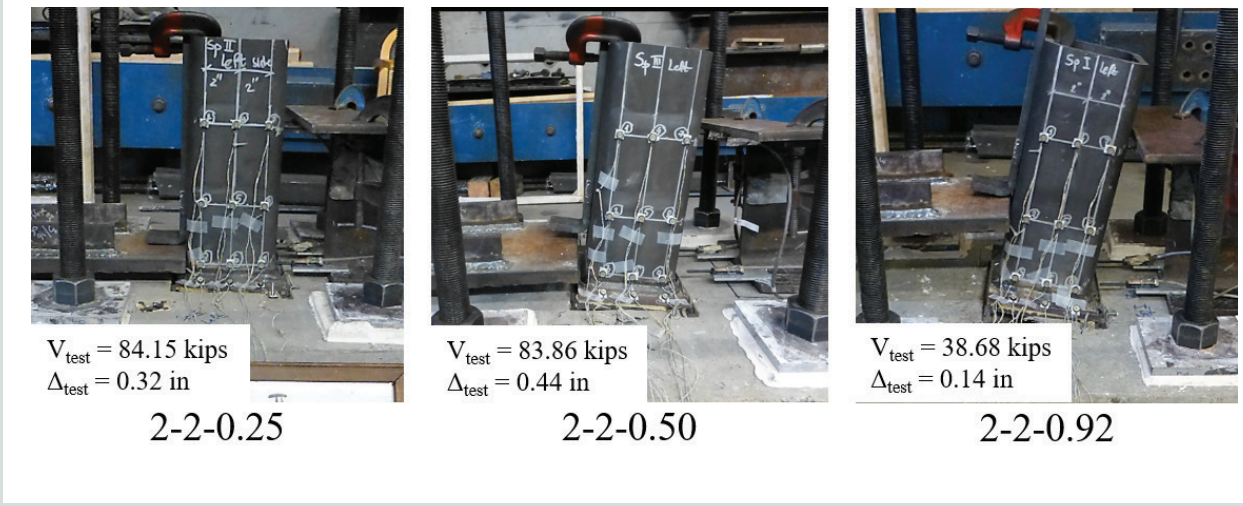

Figure 7. Photographs of specimens 2-2-0.25, 2-2-0.50, and 2-2-0.92 after failure. Note: V_{test} = total applied shear force; Δ_{test} = plate horizontal displacement at peak load. 1 in. = 25.4 mm; 1 kip = 4.448 kN.

of the plate. Specimen 2-2-0.92 had two rows of two-headed studs centered 1 in. from the north and south edges of the plate, respectively.

These three specimens were nominally identical in all other respects, and they were subjected to identical loading protocols consisting of a monotonic lateral load with load eccentricity of 5.5 in. (139.7 mm). Thus, the results presented in this section provide insight into the influence of the stud distribution on the system's response.

The global observations presented in the previous section also hold true here. The three specimens experienced a stud failure with minor damage to the concrete block, and the embed plates experienced mostly rigid body motion involving a combination of sliding and rotation. **Figures 8** and **9** show photographs of the response.

Figure 5 shows the force-displacement responses of the three specimens, and Fig. 6 compares rotation and slip. Specimen 2-0-0.92 can be regarded as the reference case, with two extra studs being added in each of the other two cases. When the studs were added to the tension side (specimen 4-0-0.92), the kinematic behavior remained almost the same (Fig. 6), suggesting that the local deformations were the same in both cases. However, specimen 4-0-0.92,

Figure 8. Lightly damaged concrete around north studs of specimen 2-0-0.92.

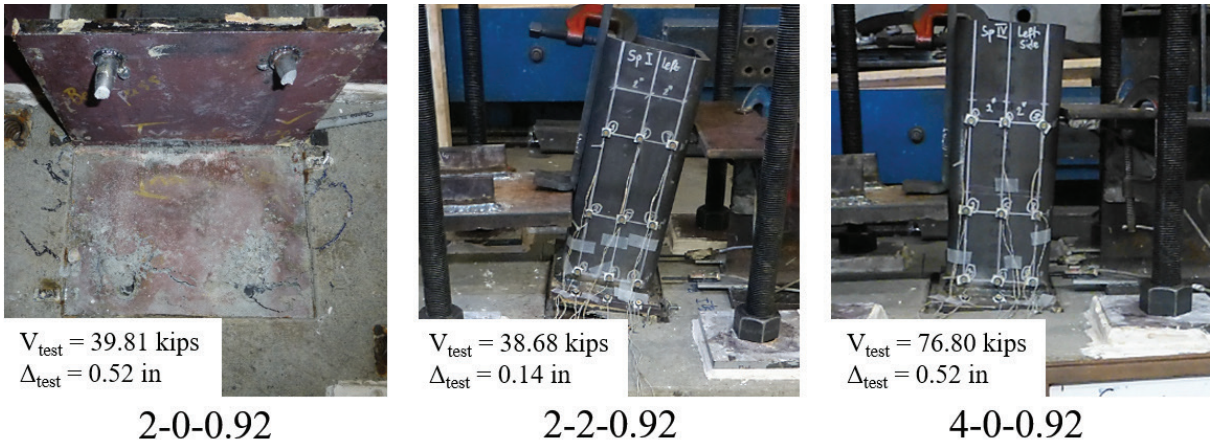

Figure 9. Photographs of specimens 2-0-0.92, 2-2-0.92, and 4-0-0.92 after failure. Note: V_{test} = total applied shear force; Δ_{test} = plate horizontal displacement at peak load. 1 in. = 25.4 mm; 1 kip = 4.448 kN.

with twice the number of studs of specimen 2-0-0.92, had essentially twice the strength (Fig. 5). This suggests that the lever arm for the bending moment remained the same, but the forces doubled. By contrast, when two studs were added to the compression side (specimen 2-2-0.92), the strength barely changed but the amount of slip decreased and the rotation increased. This suggests that in both cases the strength was controlled by flexure, which in turn was controlled by the tension strength of the upstream studs, while the downstream studs (those farthest from the actuator), were effective in inhibiting slip but were most likely not fully stressed. Specimen 2-2-0.92 showed more rotation but less slip than specimen 2-0-0.92; whether this behavior is classified as more or less ductile depends on whether slip or rotation is used as the basis of ductility.

Evaluation of experimental results

Resisting mechanisms

Figure 10 shows a free-body diagram of a headed stud connection. Equilibrium requires that both a shear force and a bending moment be transferred across the steel-to-concrete interface.

The transfer of forces occurs through a series of resisting mechanisms. The bending moment causes the plate to rotate, resulting in elongation and tension force in the studs. The tension in the studs is equilibrated by compression in the concrete and that couple provides the required flexural resistance. The mechanism could contain additional complexities, such as bending of the plate and even compression in some of the studs, but they were not seen in the experiments and are excluded from this discussion in the interest of simplicity.

The shear force is transferred through a combination of mechanisms, including shear in the studs, friction, possibly some cohesion between the steel plate and the concrete, and bearing on the concrete at the downstream end of the plate.

The studs bear against the adjacent concrete, which fails locally, typically near the surface where the local bearing stress is highest. If the studs are very shallowly embedded, they have been found by previous investigators to cause a concrete failure (for example, a pryout mechanism); otherwise, a steel failure in the stud (typically due to a combination of shear and axial tension, possibly accompanied by local kinking) is more likely to occur.

The response of the system in Fig. 10 is quite complex and involves a series of mechanisms that are difficult to quantify and simulate. The following analysis of the resisting mechanisms is intended to provide a better understanding of the overall response of the system to different load eccentricities and stud arrangements.

Analysis of experimental results

The specimens tested were designed and instrumented to minimize the number of uncertainties while isolating the desired parameters. The studs' properties and the reinforcement layout were selected to prevent a concrete failure. In addition, a foam-filled gap was introduced between the end of the plate and the adjacent concrete to eliminate any bearing resistance there. Finally, the concrete-to-plate interface was extremely smooth and cohesion contributions were likely negligible; the clean postfailure surfaces support this assumption. Thus, the experimental results could be analyzed by focusing on the behavior of the headed studs alone.

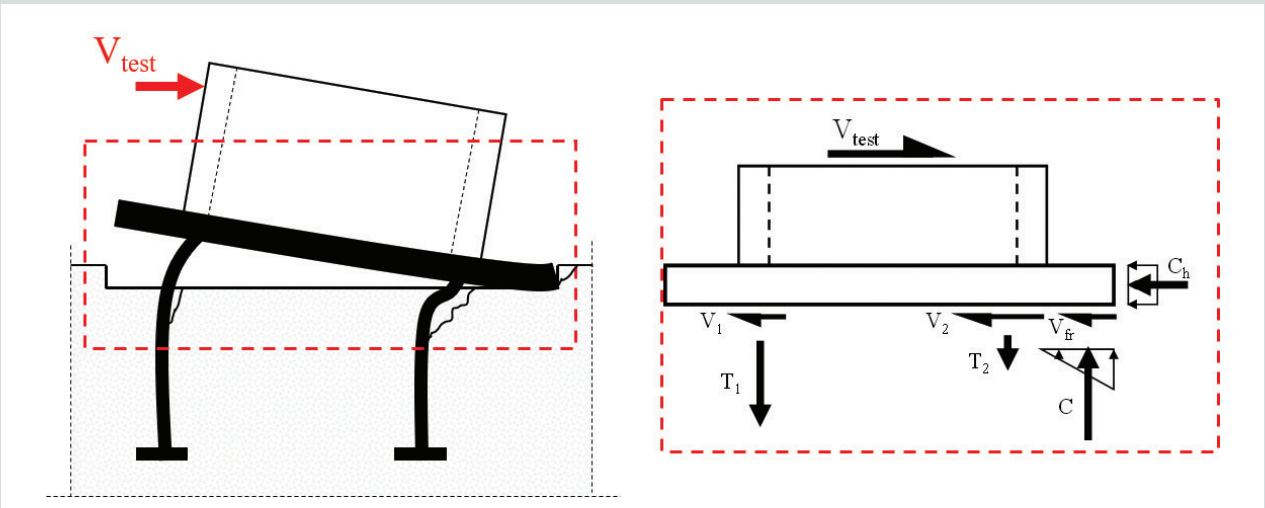

Figure 10. Connection schematic overview and embed plate free-body diagram. Note: C = compression force; C_h = horizontal bearing force due to contact between concrete and side of the plate; T_1 = tensile force in row 1 of studs; T_2 = tensile force in row 2 of studs; V_1 = shear force in row 1 of studs; V_2 = shear force in row 2 of studs; V_{fr} = shear strength due to friction; V_{test} = total applied shear force.

Any stud group must satisfy moment and shear equilibrium, which are given in Eq. (1) to (5).

$$M_{test} = V_{test}\, e \tag{1}$$

$$M_{test} = \sum T_i\, d_i \tag{2}$$

$$V_{test} = V_{fr} + \sum V_i \tag{3}$$

$$C = \Sigma T_i \tag{4}$$

$$V_{fr} \le \mu C \tag{5}$$

where

M_{test} = applied moment

V_{test} = applied shear force

e = load eccentricity

T_i = tension force in stud row i

d_i = distance of studs in row i from embed plate edge

V_{fr} = shear strength due to friction

V_i = dowel shear in stud row i

C = compressive force between plate and concrete

μ = coefficient of sliding friction

Failure will occur in flexure when the horizontal load reaches V_{flex}, which is given in Eq. (6).

$$V_{flex} = \frac{M_n}{e} = \frac{\sum d_i T_i}{e} = \frac{d_{res} \sum T_i}{e} \tag{6}$$

where

V_{flex} = shear strength associated with flexural failure

M_n = nominal flexural strength

d_{res} = lever arm of the resultant tension force of all the studs

Failure will occur in a combination of shear and flexure when the horizontal load reaches V_{shear}, which is given in Eq. (7).

$$V_{shear} = \sum V_i + \mu \sum T_i \tag{7}$$

where

V_{shear} = shear strength associated with shear failure

However, in general, there are too many unknowns to permit a unique solution for the shear strength using equilibrium alone. In the special case of high eccentricities, e will be large so V_{flex} will be small. Then, for Eq. (6) and (7) to give the same value, the dowel forces V_i will be zero and the friction demand may be less than the friction capacity based on μ. Then the equations may be combined to give the following:

$$\frac{e\mu}{d_{res}} \ge 1.0 \tag{8}$$

This is the condition that shows when the failure is controlled by pure flexure, and it is similar in principle to the findings of Mattock et al.[16]

For the specimens with one row of studs, $d_{res} = d_1 = 6$ in. (152.4 mm), and $e/d_1 = 0.92$. The use of ACI's value of $\mu = 0.70$ leads to $e\mu/d_{res} = 0.64 < 1.0$, so the failure was controlled by a combination of shear and flexure for which both friction and dowel action must be present. This can be confirmed by separately evaluating V_{flex} and V_{shear} for specimen 2-0-0.92 using the measured strength of the stud steel. If both studs are assumed to resist tension alone, as is assumed in the shear friction theory, the total tension force is $\sum T_i = 2 \times 0.31$ in.^{2} $\times$ 81 ksi = 49.7 kip (221 kN). The bending strength of the connection is then $M_n = d_1 \times T_n$, (where T_n is the tensile force in the nth row of studs), and the corresponding horizontal strength based on flexure is $V_{flex} = M_n/e = 54.2$ kip (241 kN). The horizontal strength based on shear V_{shear}, that is, the maximum friction force, is μT_n, or $0.7 \times 49.7 = 34.8$ kip (155 kN). This is less than V_{flex}, so the specimen would be controlled by V_{shear}, or 34.8 kip. However, the measured shear force at failure was 39.2 kip (174 kN), or 13% larger than the V_{shear} calculated by shear friction. Because the calculated values were obtained using the measured tension strength of the stud steel, the only possible explanations are that either the friction coefficient was 0.79 (that is, significantly higher than reported by other investigators) or that the shear resistance was provided by a combination of friction and stud shear. It is believed that the latter occurred here. Consideration of specimen 4-0-0.92 leads to an almost identical conclusion.

For the connections with two rows of studs, $d_{res} = 3.5$ in. (88.9 mm). With μ assumed to be 0.70, Eq. (8) shows that e must be greater than 5 in. (127 mm) for the specimen to be flexure controlled. Only specimen 2-2-0.92 satisfied this condition, with $e = 5.5$ in. (139.7 mm). Some slip did occur in it, but as Fig. 6 shows, the ratio of rotation to sliding distance was much larger than for any other specimen. This suggests that μ was probably less than 0.70, in which case the specimen was on the borderline between a mixed failure and a pure flexural failure.

In all cases other than $\mu e/d_{res} > 1.0$, the problem is statically indeterminate. If n_{row} rows of studs are used, the connection is n_{row} degrees indeterminate. For a single row of studs, it is one degree indeterminate, with the only outstanding question being how the horizontal load is shared between the shear force in the studs and friction. For $n_{row} > 1$, the unknowns not only include the distribution between stud shear and friction but also the distribution among the different rows of studs. In practice, the great majority of embedded plates will be

furnished with a symmetric pattern of studs placed in two or more rows and they will therefore be indeterminate.

Previous modeling efforts for flexure-shear interaction have distributed the shear force somewhat arbitrarily, rather than solving the indeterminate problem. For example, PCI recommends using "engineering judgment" to assign the shear and tension forces among the studs, and ACI 318-14 gives a choice of using either pure shear friction (section 22.9) or dowel action (chapter 17), albeit with a tension-shear interaction provision.

It should be noted that the indeterminate problem is not an easy one. At failure, the studs are no longer elastic, so the normal methods of elastic indeterminate analysis cannot be used. It is also possible that the friction coefficient might change during the loading, either because of progressive changes in the roughness of the surfaces or because shrinkage might have led to a slight separation between the two surfaces before the load was applied and thus have caused a delay in the start of the frictional resistance. The nonlinearity of the rotation-slip curves in Fig. 4 also suggests that the relative contributions of the two mechanisms may not be constant throughout the loading. Further reasons for changing contributions to the tension and shear forces include local crushing of the concrete where the studs bear on it and the fact that the stress-strain curve of the stud steel is nonlinear.

It is evident that an interaction exists between the moment and shear applied to the connection. The measured strengths were normalized by dividing by V_{flex} and V_{shear} from Eq. (6) and (7) and are given in **Table 3** and plotted in **Fig. 11**. Figure 11 also plots a simple interaction curve based on Eq. (9) for values of the exponent m = 1, 2, and 3.

$$\left(\frac{V_{test}}{V_{flex}}\right)^m + \left(\frac{V_{test}}{V_{shear}}\right)^m = 1 \qquad (9)$$

The individual test results may be identified from the values in the table and the resulting e/d_{res}. On the plot, the slope of each radial line is equal to e/d_{res}. Four of the test points lie reasonably close to an interaction curve with m = 2. The fifth (specimen 2-2-0.92) gives results that appear to be anomalously low in that the V_{test} value is smaller than would be needed to match the interaction curve. It is believed that some error must have occurred with that test because the measured strength for that specimen (2-2-0.92) with four studs was less than that of specimen 2-0-0.92 with only two studs (38.68 kip [172 kN] compared with 39.34 kip [175 kN]). While the interaction equation (Eq. [9]) provides a promising basis, more experimental data are clearly needed to calibrate it properly.

Conclusion

The purpose of this experimental program was to investigate the effects of load eccentricity and stud distribution on the response of headed stud connections. Although these connections in real applications are always subjected to combined shear and moment demands, experimental data pertaining to such combined loading are scarce in the literature.

The findings from the experimental program and the analysis support the following conclusions:

- Headed stud connections subjected to bending and shear resist loads through a series of complex mechanisms that are difficult to isolate and model. The applied shear is resisted partly by dowel action of the studs and partly by a frictional force that arises at the steel-to-concrete interface

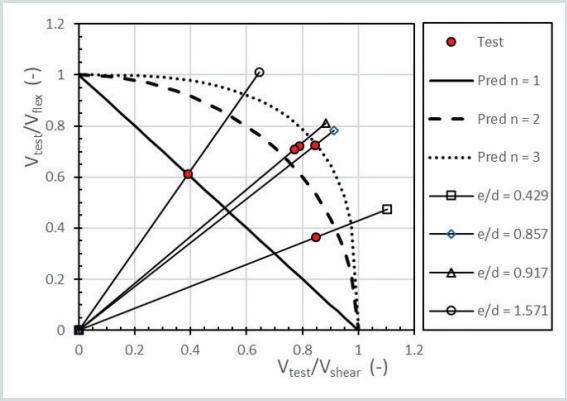

Figure 11. Interaction diagram for normalized shear strengths. Note: d = lever arm; e = load eccentricity; V_{flex} = shear strength associated with flexural failure; V_{shear} = shear strength associated with shear failure; V_{test} = total applied shear force.

Table 3. Normalized test results

Specimen ID	n_1	n_2	e, in.	V_{test}, kip	V_{test}/V_{flex}	V_{test}/V_{shear}
2-0-0.92	2	0	5.5	39.20	0.723	0.789
4-0-0.92	4	0	5.5	76.80	0.708	0.773
2-2-0.92	2	2	5.5	38.68	0.611	0.389
2-2-0.50	2	2	3.0	83.86	0.723	0.844
2-2-0.25	2	2	1.5	84.15	0.363	0.847

Note: e = load eccentricity; n_1 = number of studs in row 1; n_2 = number of studs in row 2; V_{flex} = shear strength associated with flexural failure; V_{shear} = shear strength associated with shear failure; V_{test} = total applied shear force applied in test. 1 in. = 25.4 mm; 1 kip = 4.448 kN.

due to the bending-induced compression; the moment applied to the connection is resisted by tension in the studs and compression at the steel-to-concrete interface.

- Any moment applied concurrently with the shear has the potential to affect the shear strength. Codes currently offer no formal guidelines for interaction of the two effects. Mattock et al.[16] idealized all connections as being either shear controlled or moment controlled, but this appears to oversimplify the problem. A simple interaction equation offers a possible relationship that describes contributions of each behavior that are continuous functions of the eccentricity of the load.

- In most cases, shear force demands are resisted by both dowel action of the studs and friction. Current design models fail to acknowledge this and attribute all the resistance to one mechanism or the other. However, the test results show that these idealizations cannot be correct.

- Only in the simple case of a single row of studs and $\mu e / d_{res} > 1$ is the system statically determinate and the applied shear resisted by friction alone. Then the studs resist pure tension and no slip occurs. In all other cases, the system is statically indeterminate and the shear demand is shared between the friction and dowel action mechanisms.

Acknowledgments

This research was conducted with the sponsorship of PCI under the auspices of the Daniel P. Jenny fellowship. The authors wish to thank Roger Becker, formerly of PCI; Harry Gleich of Metromont Corp.; Ned Cleland of Blue Ridge Design Inc.; and Neil Hawkins, who served as advisors to this project. Their assistance and input are greatly appreciated.

References

1. Viest, I. M. 1956. "Investigation of Stud Shear Connectors for Composite Concrete and Steel T-Beams." *ACI Journal* 27 (8): 875–891.

2. Buttry, K. E. 1965. "Behavior of Stud Shear Connectors in Lightweight and Normal Weight Concrete." Report 68-6. Columbia, MO: Missouri Cooperative Highway Research Program, Missouri State Highway Department, and University of Missouri.

3. Baldwin Jr., J. W., J. R. Henry, and G. M. Sweeney. 1965. "Study of Composite Bridge Stringers—Phase II." Technical report. Department of Civil Engineering, University of Missouri, Columbia, MO.

4. Hawkins, N. M. 1971. "The Strength of Stud Shear Connectors." Research report R141. Sydney, Australia: Department of Civil Engineering, University of Sydney.

5. Ollgaard, J. G., R. G. Slutter, and J. W. Fisher. 1971. "Shear Strength of Stud Connectors in Lightweight and Normal-Weight Concrete." *Engineering Journal* 8 (2): 55–64.

6. Hawkins, N. M., and D. Mitchell. 1984. "Seismic Response of Composite Shear Connections." *Journal of Structural Engineering* 110 (9): 1–10.

7. Anderson, N. S., and D. F. Meinheit. 2005. "Pryout Capacity of Cast-In Headed Stud Anchors." *PCI Journal* 50 (2): 90–112.

8. AISC (American Institute of Steel Construction). 2017. *Manual of Steel Construction: Load and Resistance Factor Design*. 15th ed. Chicago, IL: AISC.

9. Anderson, N. S., and D. F. Meinheit. 2007. "A Review of Headed-Stud Design Criteria in the Sixth Edition of the *PCI Design Handbook*." *PCI Journal* 52 (1): 82–100.

10. PCI Industry Handbook Committee. 2010. *PCI Design Handbook: Precast and Prestressed Concrete*. MNL-120. 7th ed. Chicago, IL: PCI.

11. Gomez, I. R., A. M. Kanvinde, and G. G. Deierlein. 2011. "Experimental Investigation of Shear Transfer in Exposed Column Base Connections." *Engineering Journal* 48: 246–264.

12. AASHTO (American Association of State Highway and Transportation Officials). 2012. *AASHTO LFRD Bridge Design Specifications*. 6th ed. Washington, DC: AASHTO.

13. ACI (American Concrete Institute) Committee 318. 2014. *Building Code Requirements for Structural Concrete (ACI 318-14) and Commentary (ACI 318R-14)*. Farmington Hills, MI: ACI.

14. Pallarés, L., and J. F. Hajjar. 2010. "Headed Steel Stud Anchors in Composite Structures, Part I: Shear." *Journal of Constructional Steel Research* 66 (2): 198–212.

15. AWS (American Welding Society). 2015. *Structural Welding Code—Steel*. AWS D1.1/D1.1M:2015. Miami, FL: AWS.

16. Mattock, A. H., L. Johal, and H. C. Chow. 1975. "Shear Transfer in Reinforced Concrete with Moment or Tension Acting Across the Shear Plane." *PCI Journal* 20 (4): 76–93.

Notation

C = compression force normal to the plate-to-concrete interface (force)

C_h = horizontal bearing force due to contact between concrete and side of the plate

d_1 = distance of studs in rows 1 from embed plate edge

d_2 = distance of studs in rows 2 from embed plate edge

d_i = distance of studs in row i from embed plate edge

d_{res} = lever arm of the resultant tension force of all studs

d_s = stud diameter

e = load eccentricity

f_c' = concrete compressive strength

f_{peak} = peak tensile stress of studs obtained from tension test

f_{uta} = ultimate tension strength of stud anchor reinforcement

f_y = stud yield stress obtained from tension test

h_s = stud length

m = interaction equation exponent

M = flexural demand on precast connection

M_n = nominal flexural strength

M_{test} = total applied bending moment applied in test

n_i = number of studs in row i

n_{row} = number of rows of studs

T = tensile force normal to the plate-to-concrete interface

T_i = tensile demand in row i of studs (force)

V = shear demand on precast connection

V_{flex} = shear strength associated with flexural failure

V_{fr} = shear strength due to friction

V_i = shear demand in row i of studs (force)

V_{shear} = shear strength associated with shear failure

V_{test} = total applied shear force applied in test

w_u = separation between steel plate and concrete at ultimate shear load

α_u = plate rotation at ultimate shear load (rad)

Δ_{test} = plate horizontal displacement at peak load

μ = coefficient of friction

About the authors

Otgonchimeg Davaadorj is a former master's degree student in structural engineering in the Department of Civil and Environmental Engineering at the University of Washington in Seattle.

Paolo M. Calvi, PhD, is an assistant professor in the Department of Civil and Environmental Engineering at the University of Washington.

John F. Stanton, PhD, PE, is a professor in the Department of Civil and Environmental Engineering at the University of Washington.

Abstract

An experimental study on five specimens, representative of precast concrete beam-to-column joints, was conducted to investigate the behavior of headed stud connections subjected to combined shear and bending. The variables were the load eccentricity and the headed stud distribution. During each experiment, shear and normal stresses across the steel-to-concrete interface and the resulting horizontal and vertical displacements were continuously monitored. As intended, all specimens failed along the steel-to-concrete interface because of stud yielding or fracturing. The results demonstrate that both variables investigated influence the response of the system and that estimating the correct distribution of shear and bending actions between the studs is a problem that should be further investigated.

Keywords

Eccentric load, headed stud, joint, shear strength, steel-to-concrete interface behavior.

Review policy

This paper was reviewed in accordance with the Precast/Prestressed Concrete Institute's peer-review process.

Reader comments

Please address any reader comments to *PCI Journal* editor-in-chief Tom Klemens at tklemens@pci.org or Precast/Prestressed Concrete Institute, c/o *PCI Journal*, 8770 W. Bryn Mawr Ave., Suite 1150, Chicago, IL 60631.